ELSEVIER

Polymer Vol. 37 No. 14, pp. 3065–3078, 1996

0032-3861/96/$15.00 + 0.00

Compatibilizing effect of a maleic anhydride functionalized SEBS triblock elastomer through a reaction induced phase formation in the blends of polyamide 6 and polycarbonate: 1. Morphology and interfacial situation

S. Horiuchi*, N. Matchariyakul†, K. Yase and T. Kitano
National Institute of Materials and Chemical Research, 1-1, Higashi, Tsukuba, Ibaraki, Japan

and H. K. Choi and Y. M. Lee
National Industrial Technology Institute, 2, Joogang-Dong, Kwachun, Kyungi-Do, Korea
(Received 4 September 1995; revised 17 November 1995)

The result of a study on the effect of poly[styrene-*b*-(ethylene-*co*-butylene)-*b*-styrene] triblock copolymer functionalized by maleic anhydride (SEBS-gMA) on the morphology and interface of the incompatible polymer blends of polyamide 6 (PA6) and polycarbonate (PC) is presented. The electron spectroscopic imaging with transmission electron microscopy was introduced to investigate the morphological features and interfacial situation of these blends. It has been found that the functionalized SEBS is dispersed in PA6 phase at about 50 nm in diameter and also exists on the domain boundary of PA6 and PC to envelope the PC domains in the blends with a matrix of PA6, while the unmodified SEBS attaches to PC particles but does not surround the domains. This means that the *in situ* reaction between PA6 and SEBS-gMA during mixing induces the envelop formation of SEBS on PC domains. The formation of SEBS-gMA phase on the interface works as a coupling agent to improve interfacial adhesion between PA6 and PC, which leads to the disappearance of voids on the domain boundary generated due to the different volume shrinkage between PA6 and PC in fast cooling in a mould. In the PC rich blends, SEBS-gMA is occluded in PA6 domains and exists on the interface between PA6 and PC, while with unmodified SEBS the dispersed SEBS and PA6 phases form separate dispersed phase in PC matrix. Dynamic mechanical analysis has revealed that the glass transition temperatures (T_gs) of PA6 and PC phases in the blends are slightly lower than the respective pure polymers and that the incorporation of SEBS-gMA does not affect the T_gs of each phase. This indicates that chemical reactions between PA6 and PC during melt mixing, which produce low molecular weight species of PC occurred regardless of the incorporation of SEBS-gMA and that SEBS-gMA on the domain boundary is not miscible enough to reside within the PC domains. Copyright © 1996 Elsevier Science Ltd.

(Keywords: compatibilizer; polyamide 6; polycarbonate)

INTRODUCTION

Polyamide 6 (PA6) and polycarbonate (PC) are thermodynamically immiscible and incompatible in whole temperature and in whole composition ranges. Blends of PA6 and PC have been investigated in a full range of composition by Gattiglia *et al.*[1–4]. They have reported that the mixtures are characterized by domains of clearly segregated homophases and voids between the two polymers. Moreover, chemical reactions between the two polymers give rise to low molar mass compounds which leads to poor mechanical properties. When immiscible polymers are mixed, the interfacial adhesion is weak which results in inferior mechanical properties and poor dispersion of the components. Therefore, compatibilizing agents are required to achieve satisfactory interfacial adhesion and interfacial compatibility which lead to high performance materials.

PA6 and PC are important commercial polymers, each providing outstanding performance in a variety of applications. Nevertheless, they present some negative aspects that are in some ways asymmetrical: PA6 is strongly resistant to most solvents while PC is not; PC is insensitive to moisture and durable to various weathering conditions while PA6 greatly suffers from humidity. Hence, PA6/PC blends are expected to complement each disadvantage while maintaining the good properties of each polymer.

PA-based immiscible blends were compatibilized by reactive polymers[5–12]. Reactive compatibilizers with anhydride form a chemical linkage through the reaction

* To whom correspondence should be addressed
† Permanent address: Technology and Environmental Service, Rama 6 Road, Bangkok 10400, Thailand

of anhydride groups with the polyamide end groups. This reaction causes the graft copolymer which enhances the interfacial compatibility of immiscible polymer blends. Maleic anhydride (MA) is a typical reagent used to functionalize polyoefins[13]. Blends of poly(propylene) (PP)/nitrile rubber[7], high density polyethylene (HDPE)/PA6[8], and PP/PA[9–12] were compatibilized by maleation of the respective hydrocarbon components.

The work described here is an attempt to incorporate a functionalized triblock elastomer as a reactive compatibilizer into blends of PA6 and PC. Blends of a polyamide with a maleated styrene-based triblock copolymer having a hydrocarbon mid-block (SEBS-gMA) have been introduced as a super tough nylon and have been investigated scientifically[14–19]. This functionalized copolymer reacts with the polyamide during melt processing, which results in chemical coupling of the phases and reduction of the dispersed rubber particle size.

EXPERIMENTAL

Materials

All materials used in this work are supplied from commercial sources. PA6 is a hydrolytic poly-(ϵ-caprolactam), product name A1030BRF, supplied by Unichika Co. Ltd with a number average molecular weight of 22 500 and a melting flow rate of 4.3. The concentration of amine end group was determined at 5.0×10^{-5} mol g^{-1} by titration. Bisphenol-A PC was supplied by Teijin Chemical Co. Ltd, product name Panlite L-1250Y. These two polymers were dried at 80°C for at least 12 h in a vacuum oven to remove sorbed water before processing. The triblock copolymer of poly[styrene-*b*-(ethylene-*co*-butylene)-*b*-styrene] (SEBS) is incorporated into the blends of PA6 and PC for compatibilizing of this system. This copolymer has styrene end blocks and a hydrogenated butadiene midblock resembling an ethylene/butylene copolymer. The SEBS functionalized with 2 wt % MA onto the hydrocarbon chains, designated SEBS-gMA, is Kraton 1901, supplied by Shell, molecular weight 20 000, styrene content 29 wt %. Unmodified SEBS is Kraton 1652, molecular weight and styrene contents the same as those of Kraton 1901.

Blending procedures

PA6 and PC were mixed using the compact mixing machine developed in our laboratory. The mixing part of this machine is illustrated in *Figure 1*. PA6 and PC (10 g in total) with different amounts of SEBS-gMA or SEBS were placed into the mixing chamber and were mixed with the screw at a rotation speed of 80 rpm at 260°C for 10 min. A blended sample was then injected into a mould placed just below the machine. The moulded sheet is 3 mm in thickness. The composition of PA6/PC was held at 25/75, 50/50 and 75/25, while the amount of added SEBS-gMA or SEBS was varied from 5 phr (5 g against 100 g of the total amount of PA6 and PC) to 15 phr.

Transmission electron microscopy

Morphological studies were carried out by transmission electron microscopy (TEM). Sections were microtomed from moulded samples perpendicular to the flow direction, then stained with phosphotungstic acid (PTA) or ruthenium tetraoxide (RuO_4). Both staining agents

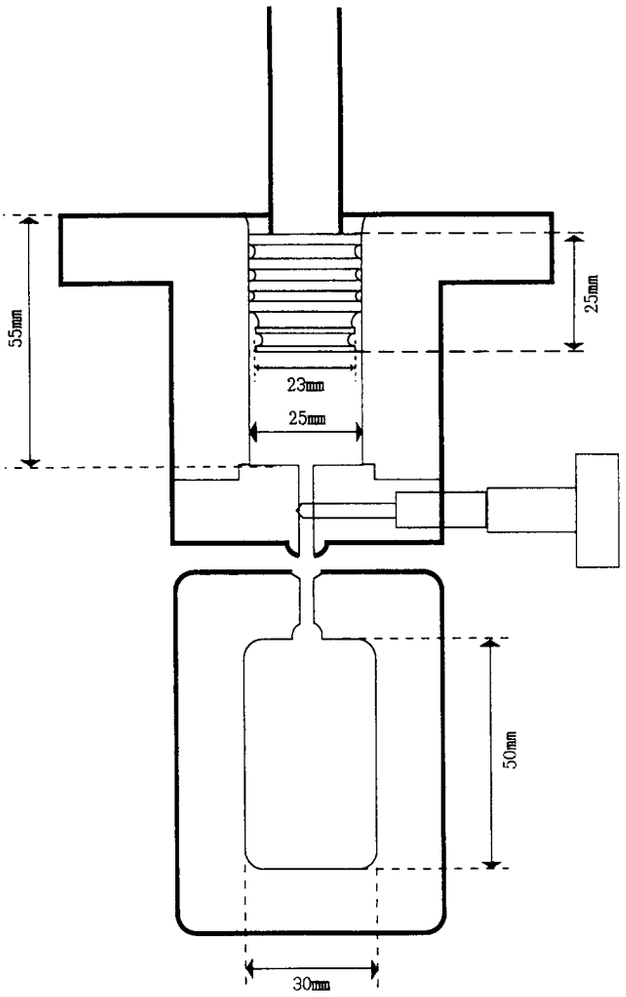

Figure 1 Schematic illustration of the mixing machine used in this work

were used as aqueous solutions of 0.5 wt% RuO_4 and 5 wt% PTA. The electron spectroscopic images (ESIs) were taken using Zeiss CEM 902 at an accelerating voltage of 80 kV which attaches an integrated electron energy loss spectrometer for electron energy loss spectroscopy (EELS). Detailed descriptions of Zeiss EM 902 have appeared elsewhere[20–23]. Images were recorded on the Imaging Plate (IP) and processing of the images was carried out with FDL5000, Fuji Photofilm Film Co., Ltd. A semi-automatic digital image analysis technique was employed to determine the size of dispersed domains from TEM photographs using an IBAS image processor. More than two hundred particles were counted and the diameter assigned to each particle was determined as that of a circle with equivalent area.

Scanning electron microscopy

Fracture surfaces of blend materials were observed with a SEM, Topcon DS-720, at an accelerating voltage of 15 kV. The samples were fractured at liquid nitrogen temperature and were coated with gold to make them electrically conducting.

Dynamic mechanical analysis

Dynamic mechanical analysis (d.m.a.) was carried out on a Seiko Instrument SDM5600 at a frequency of 10 Hz,

Figure 2 Four selective images with ESI at the different energy losses with the energy loss window of 20 eV of 75/25/10 PA6/PC/SEBS-gMA blend stained with PTA: (a) ESI at $\Delta E = 0$ eV (zero loss image); (b) at $\Delta E = 70$ eV (a contrast tuned image); (c) $\Delta E = 150$ eV (a structure sensitive image) and (d) $\Delta E = 300$ eV (above Carbon k-edge)

and at a heating rate of 2°C min^{-1}. Samples were cut out from moulded sheets at a size of 50 × 5 × 3 mm.

RESULTS AND DISCUSSION

Morphology observation by electron spectroscopic imaging

The contrast in TEM imaging is formed from the sum of elastically, inelastically and non-scattered electrons, and is enhanced by using the objective aperture to exclude the elastically scattered electrons which are scattered at wide angles. In conventional TEM, images contain contributions from non-scattered and inelastically scattered electrons that pass a specimen. ESI allows us to separate the contributions by inserting an energy selecting slit in the energy dispersive plane of a prism spectrometer. In polymer blend materials, the element composition of each component is quite similar, which would lead to low contrast without staining in conventional TEM images. Also, with thick specimens more than 50 nm, the chromatic aberration leads to diffuse images and drastically limits the resolution. Conventionally, the use of ultra-thin specimens (<50 nm) or high acceleration voltage is necessary for achieving sharp images. Through use of ESI mode, the chromatic aberration and the background are significantly reduced,

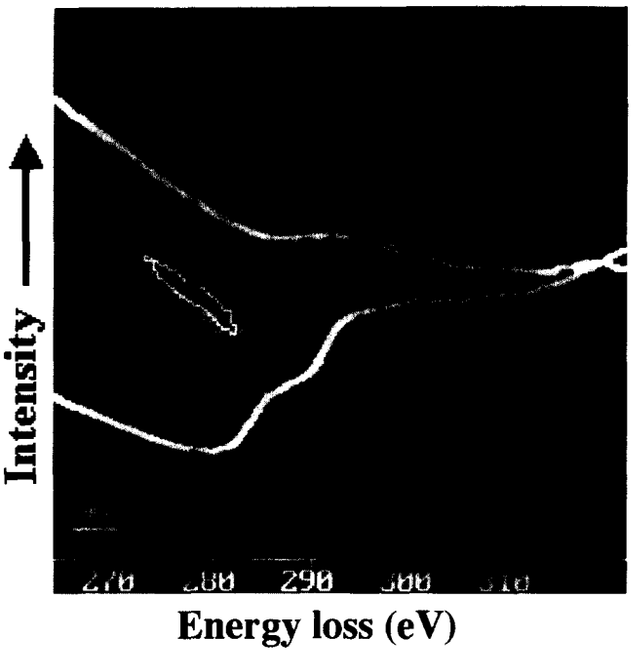

Figure 3 ESI image at $\Delta E = 270$ eV of 75/25/10 PA6/PC/SEBS-gMA blend with electron energy loss spectra of a PC domain and the phase surrounding the PC particle obtained with Image-EELS technique. The specimen has been stained with PTA

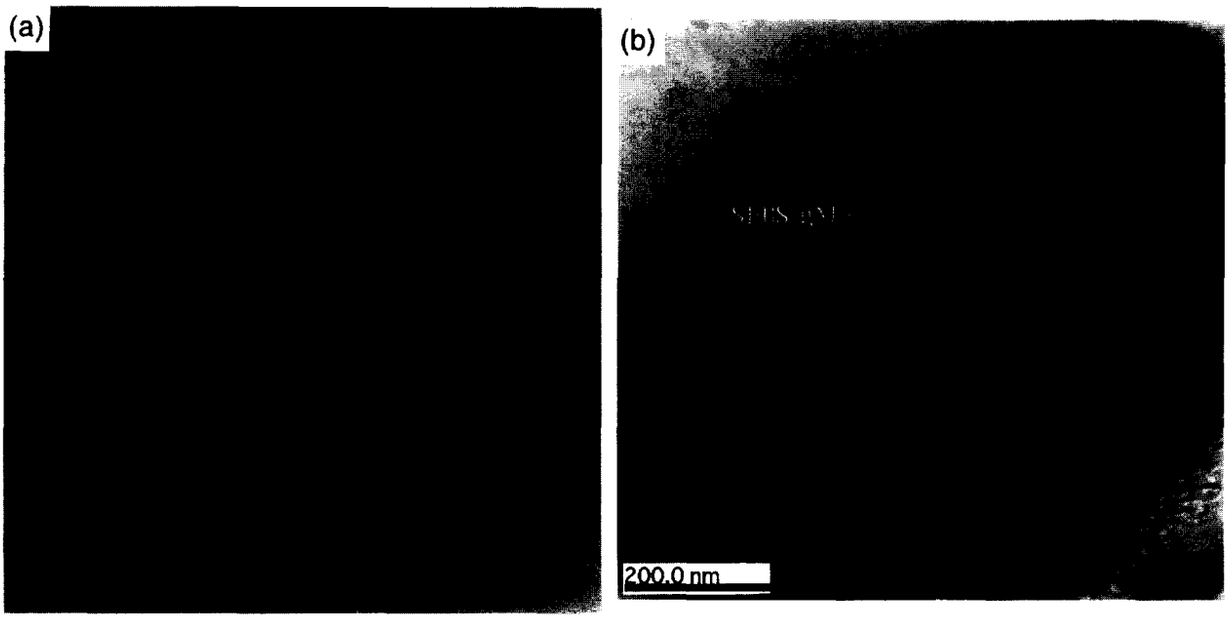

Figure 4 (a) TEM photograph of 100/10 PC/SEBS-gMA binary blend showing the dispersion of SEBS-gMA domains. (b) is a higher magnification view of the SEBS-gMA domain. RuO_4 has been introduced as a staining agent

thus sharp and highly resolved images with excellent contrast can be obtained even with thick specimens and at low accelerating voltage. Whereas the ESI technique has been extensively introduced in the observations of biological specimens[20], there seem to be few works on the application of ESI to the investigation of morphologies of polymer blends[24,25]. *Figure 2* shows four ESI images at different energy losses with the energy loss window of 20 eV obtained from the blend of PA6/PC/SEBS-gMA (75/25/10) where the PA6 phase is stained with PTA. The thickness of the specimen is approximately 200 nm. These photographs show the dispersed particles in stained PA6 matrix at the same position of the specimen. As shown in *Figure 2a*, the information on the dispersed particles and the boundaries between PA6 matrix and the particles cannot be clearly distinguished in the zero loss image ($\Delta E = 0$ eV), while maximum contrast and good separation of the phases can be obtained with $\Delta E =$ 70 eV (*Figure 2*). In the zero loss image, the stained areas become very dark and cannot be clearly identified together with much brighter areas because of the limited dynamic range of a recording media. By varying the energy loss of the electrons imaged, the contrast difference can be adjusted and smoothed out to give maximum information in all image areas. Moreover, the formation of a phase around the PC particles appears as a bright area in the images formed by the inelastically scattered electrons from 150 eV to 250 eV (*Figure 2c*). The ESI at an energy loss below the carbon K-edge at $\Delta E = 285$ eV[26] offers a structure sensitive image, which allows an image to be formed with a minimum contribution from carbon and a relatively strong contribution from the non-carbon atoms inside the phases. Beyond the carbon K-edge, however, the contribution of the carbon atoms to the image intensity increases and the contrast from the noncarbon atoms becomes very low. Thus the contrast decreases again at 300 eV as shown in *Figure 2d*. *Figure 3* shows an ESI image of a PC domain at $\Delta E = 270$ eV with EELS near the carbon K-edge (285 eV) of a PC domain and the

Figure 5 TEM photograph of 100/10 PA6/SEBS-gMA binary blend stained with RuO_4

phase which envelopes the PC domain. These spectra were obtained using the Image-EELS technique[27]. Series of energy filtered images at increasing energy losses are recorded from one area with a TV camera. In a second step the intensity of selected regions in the image is measured with an image analysis system and plotted as a function of the energy loss. This technique makes it possible to obtain EELS spectra from different objects in an image and to compare with each other. As shown in *Figure 3*, below the carbon K-edge, the spectrum intensity of the phase surrounding the PC particle, is much higher than that of PC particle. This difference of the intensity reflects the contrast between the phases as

shown in *Figure 2c*. Through using the ESI mode, the difference in element concentration in respective phases has been amplified, which leads to high contrast and fine images.

The morphologies of binary blends of PA6/SEBS-gMA and PC/SEBS-gMA

In order to identify respective phases in TEM images for heterogeneous polymer systems, several staining techniques have been introduced. For the ternary blends of PA6, PC and SEBS, two staining techniques were used. PTA has been commonly used as a staining of polyamide, while RuO_4 is a widely used staining agent for various polymers including nylon, polycarbonate and polystyrene[28]. To confirm the staining intensity by RuO_4 of the respective polymers used in this study, the morphologies of the binary blends of PA6/SEBS-gMA and PC/SEBS-gMA were observed by TEM with RuO_4 staining. *Figure 4* shows TEM photographs for a binary blend of PC with 10 phr of SEBS-gMA stained with RuO_4. Dispersed SEBS-gMA phases are strongly stained as shown in *Figure 4a* and a higher magnification view of the domains as shown in *Figure 4b* reveals that the SEBS-gMA domain has a hexagonal arrangement of cylinders of selectively stained polystyrene. *Figure 5* shows the dispersed SEBS-gMA stained with RuO_4 in PA6 matrix. This reveals, as reported by Paul *et al.*[14,17], the fine dispersion of SEBS-gMA in PA6 matrix. Although the microdomain structure can be detectable, the cylindrical microphase as observed in the PC/SEBS-gMA blends is not identified. By the grafting reaction between SEBS-gMA and the PA6, interfacial tension is reduced and steric hindrance against coalescence of SEBS domains is caused, which can reduce the particle size by over two orders of magnitude[14]. The results obtained from the observation of the morphologies stained with RuO_4 confirms that styrene blocks in SEBS is most strongly stained with RuO_4 in the ternary blends of PA6, PC and SEBS. The location of SEBS in the ternary blends, therefore, can be identified by staining with RuO_4.

Reaction induced phase formation in the ternary blends of PA6/PC/SEBS-gMA

The morphological variations with different compositions

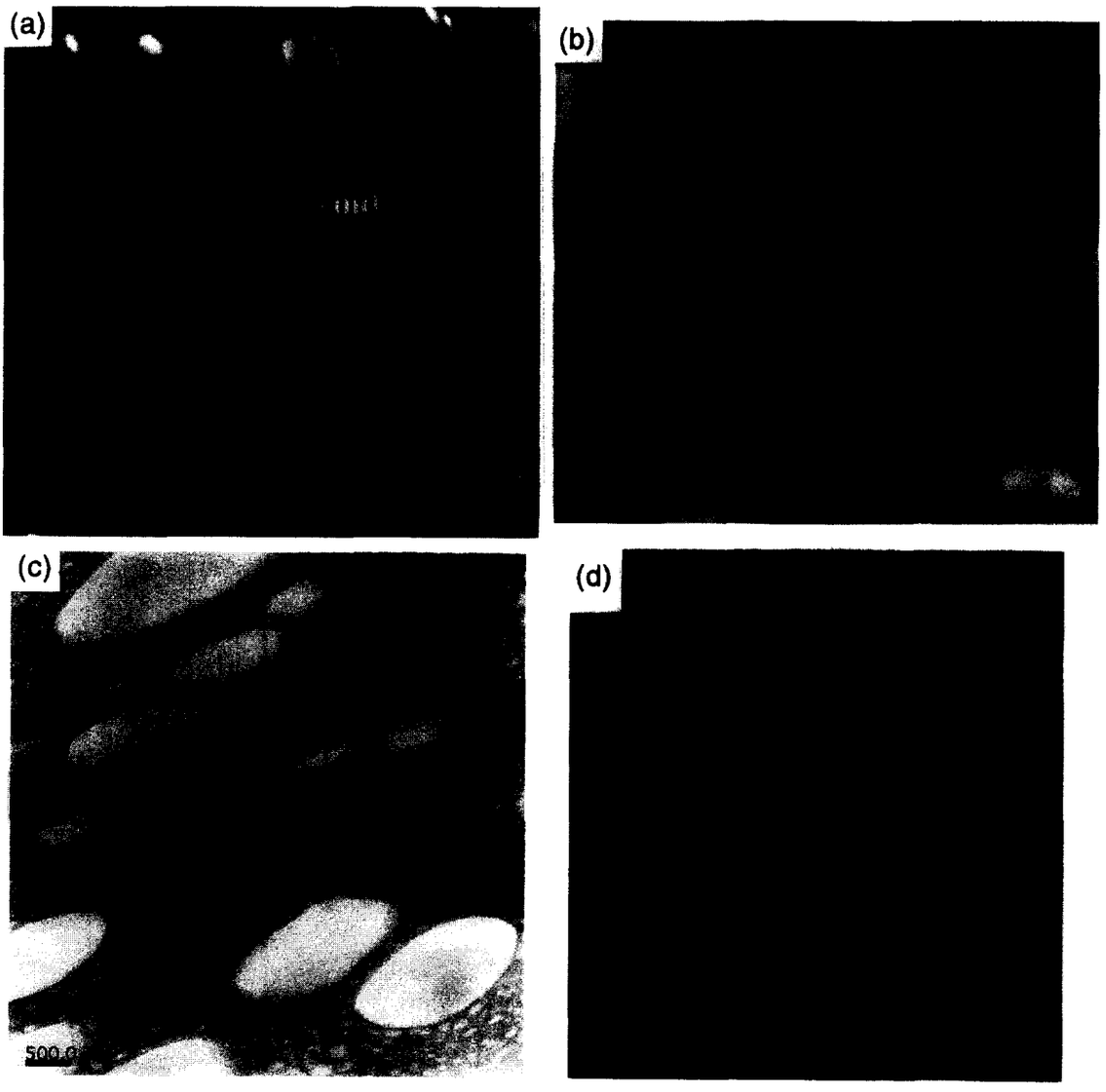

Figure 6 TEM photographs of 75/25 PA6/PC blends: (a) uncompatibilized; (b) with 5 phr; (c) 10 phr; (d) 15 phr of SEBS-gMA. PA6 phase was stained with PTA

of uncompatibilized blends of PA6/PC were investigated by Gattiglia *et al.*[2] by the observation of fracture surfaces with SEM. They reported that the blends show biphasic structures, and that voids are visible at the domain boundary. *Figure 6a* shows TEM photographs of 75/25 PA6/PC blends where PA6 matrix is stained with PTA. In TEM, electrons pass through voids without any interaction with a specimen which gives no scattered electrons. Hence, in inelastically scattered images, the darkest areas should correspond to voids. The formation of voids in the uncompatibilized blend can be explained by deferent volume shrinkage during the thermal transition of the polymers in the fast cooling in a mould. The crystallization of PA6 causes a volume decrease higher than the shrinkage of PC phase. In the uncompatibilized blends of PA6 and PC, the interfacial adhesion is so weak that delamination at the interface occurred and the voids on the domain boundary are generated.

Figure 7 TEM photograph of 75/25/10 PA6/PC/SEBS-gMA blend where SEBS-gMA domains were stained with RuO_4

Figures 6b and *6c* show the morphological changes of 75/25 PA6/PC blends by the incorporation of SEBS-gMA. These TEM photographs were taken from stained specimens with PTA. It is obvious that, by 5 phr incorporation of SEBS-gMA, the voids observed at the domain boundary in the uncompatibilized blend are not detectable. And also, small particles of which diameter is approximately 50 nm are dispersed in PA6 matrix. The number of dispersed particles in PA6 matrix is increased as the amount of SEBS-gMA is increased. *Figure 7* shows a TEM photograph taken from a specimen stained with RuO_4 of the ternary blend of 75/25/10 PA6/PC/SEBS-gMA. This reveals that the small particles dispersed in PA6 matrix are stained selectively, indicating that SEBS-gMA are dispersed in PA6 matrix. The size and structure of these particles are the same as that observed in the binary blend of PA6/SEBS-gMA as shown in *Figure 5*. This means that the reaction between maleic anhydride and PA6 to produce a graft copolymer of SEBS-gMA with PA6 occurred effectively during the blend process. *Figure 8a* shows a PC particle dispersed in the blend of 75/25/10 PA6/PC/SEBS-gMA, presenting that SEBS-gMA makes a formation of a phase surrounding the PC particles. This envelope formation of SEBS-gMA can also be observed using ESI mode with a PTA-stained specimen as shown in *Figure 8b*. It is assumed that this phase absorbs the internal stress which is generated due to the difference of thermal shrinkage between PA6 and PC, and contributes to improving the interfacial adhesion between PA6 and PC. On the other hand, no envelope formation of SEBS is observed in the blends of PA6/PC with unmodified SEBS. *Figure 9a* shows TEM

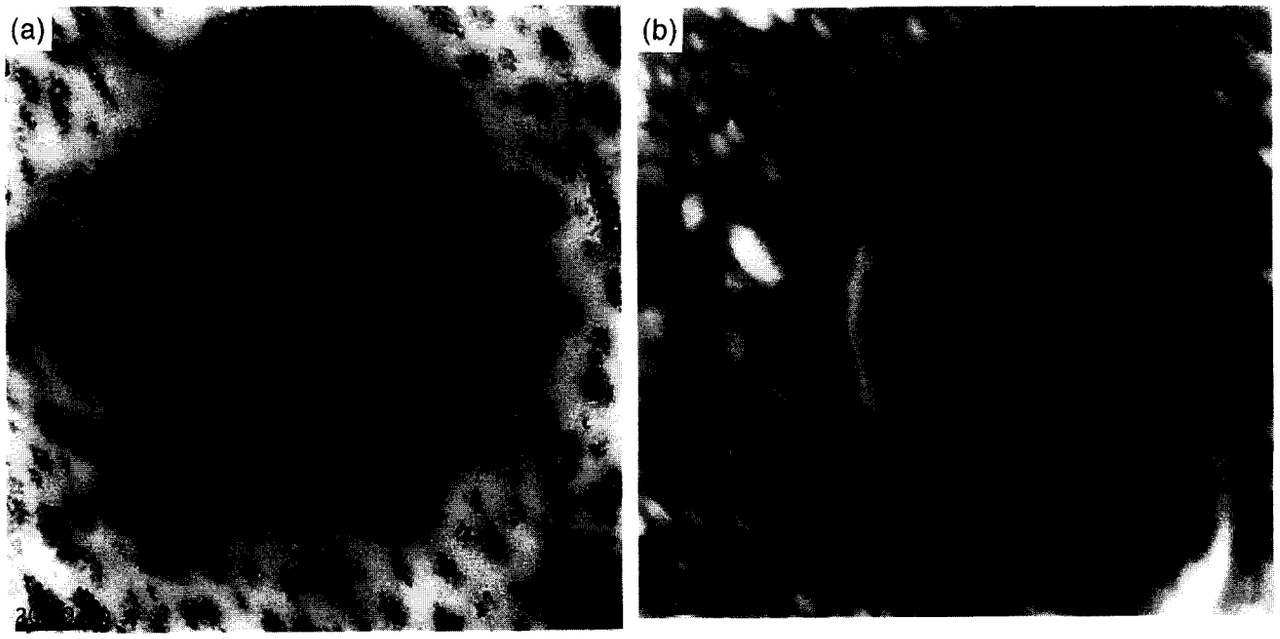

Figure 8 TEM photographs showing a dispersed PC particle in PA6 matrix in the blend of 75/25/10 PA6/PC/SEBS-gMA and presenting the envelope formation of SEBS-gMA by (a) staining with RuO_4 and (b) ESI at $\Delta E = 150$ eV, in which PA6 matrix has been stained with PTA

photographs for the ternary blends of 75/25/10 PA6/PC/SEBS where the styrene blocks of SEBS are stained with RuO_4. Here no fine dispersion of SEBS in PA6 matrix is obtained and also the photograph in higher magnification shown in *Figure 9b* reveals that SEBS domains attach to the PC domain but does not envelope the PC particles. The change of the phase formation from the attached formation to the envelope formation of SEBS emphasizes the fact that the envelope formation of SEBS-gMA on the PC particles is induced by the *in situ* reaction of SEBS-gMA to PA6.

In *Figures 10a* and *10b*, the TEM photographs in ESI mode of the blend of 50/50 PA6/PC with 10 phr SEBS-gMA taken with an energy loss of 50 eV and 100 eV respectively are presented, in which PTA has been used to stain the PA6 matrix. As same as the case of the blend series of 75/25 PA6/PC, SEBS-gMA domains exist in PA6 matrix and also envelope the PC particles. Whereas the uncompatibilized blend of 50/50 PA6/PC has been reported to show the morphology in which PC forms the matrix[1], by the addition of SEBS-gMA to the 50/50 blend, the matrix is changed from PC to PA6 by the incorporation of SEBS-gMA. This can be interpreted in terms of different melt viscosity. During the mixing process, in the blend without SEBS, the less viscous molten PA6 is masticated much better than the highly viscous PC. As a consequence, the PC constitutes the continuous matrix. By the addition of SEBS-gMA,

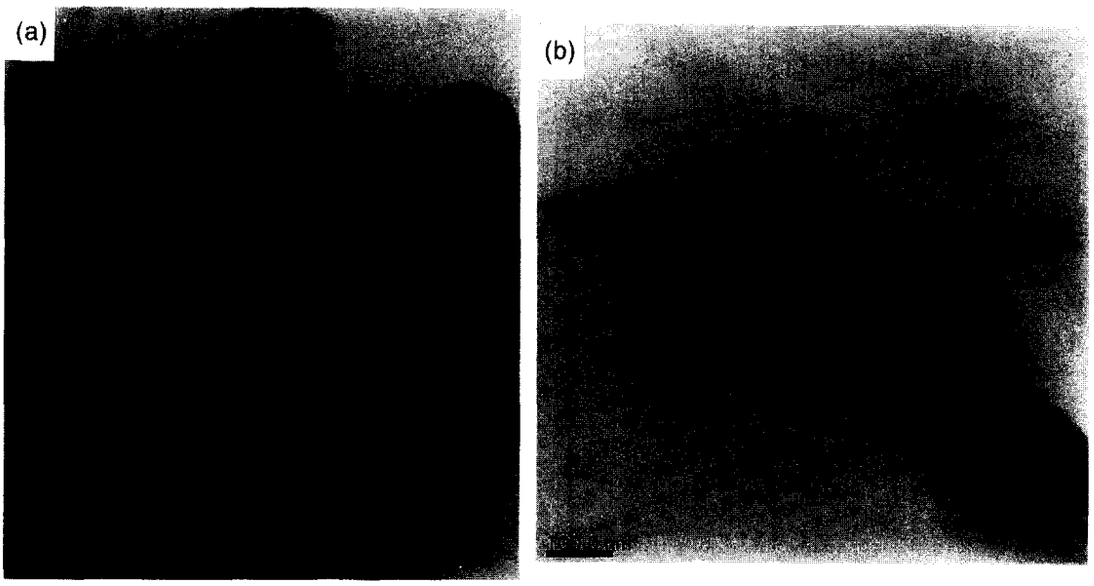

Figure 9 TEM photographs of 75/25/10 PA6/PC/SEBS. (b) is a higher magnification view of a SEBS domain attached to the PC interface. RuO_4 has been introduced to stain SEBS domains

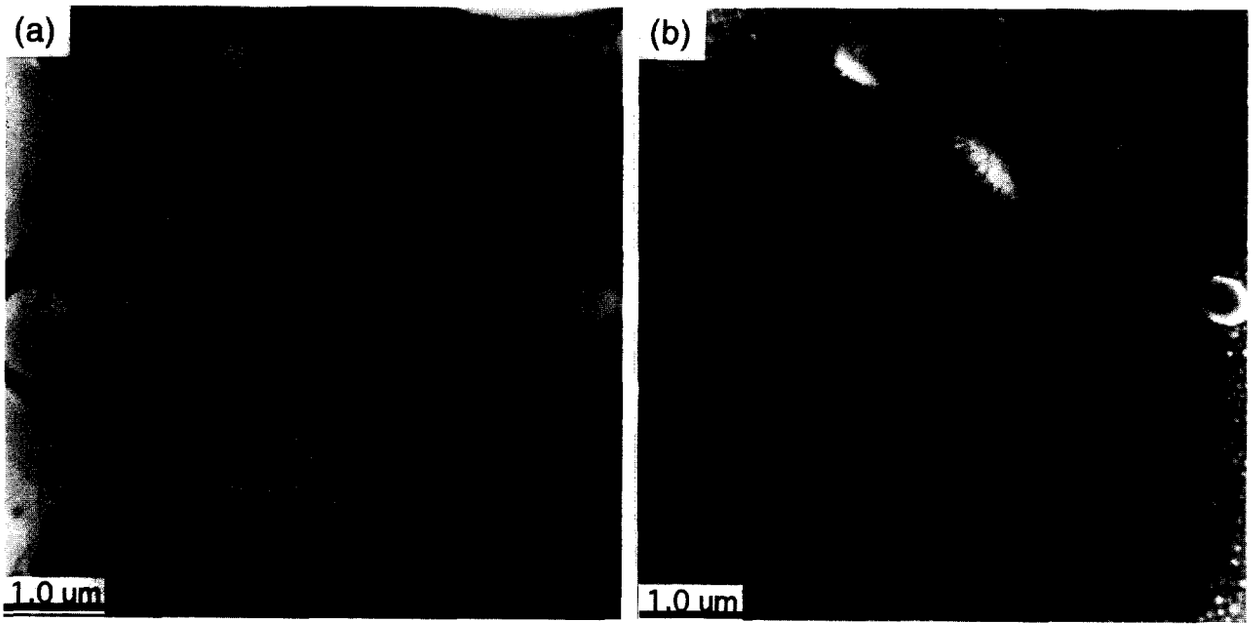

Figure 10 TEM photographs with ESI mode of 50/50/10 PA6/PC/SEBS-gMA blend: (a) ESI at $\Delta E = 50$ eV and (b) ESI at $\Delta E = 150$ eV

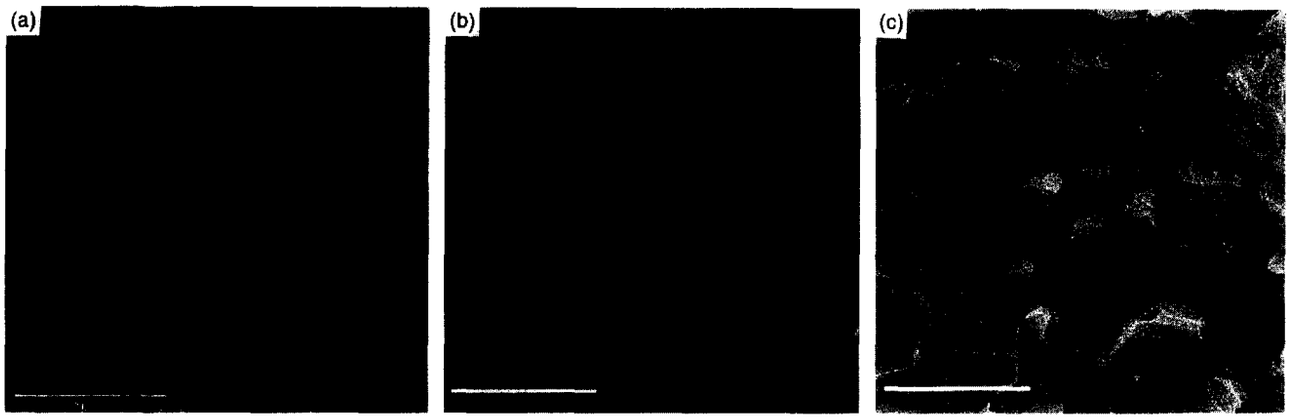

Figure 11 SEM photographs of cryogenically fractured surfaces of 75/25 PA6/PC blends: (a) uncompatibilized; (b) with 5 phr of SEBS-gMA; (c) with 5 phr of SEBS

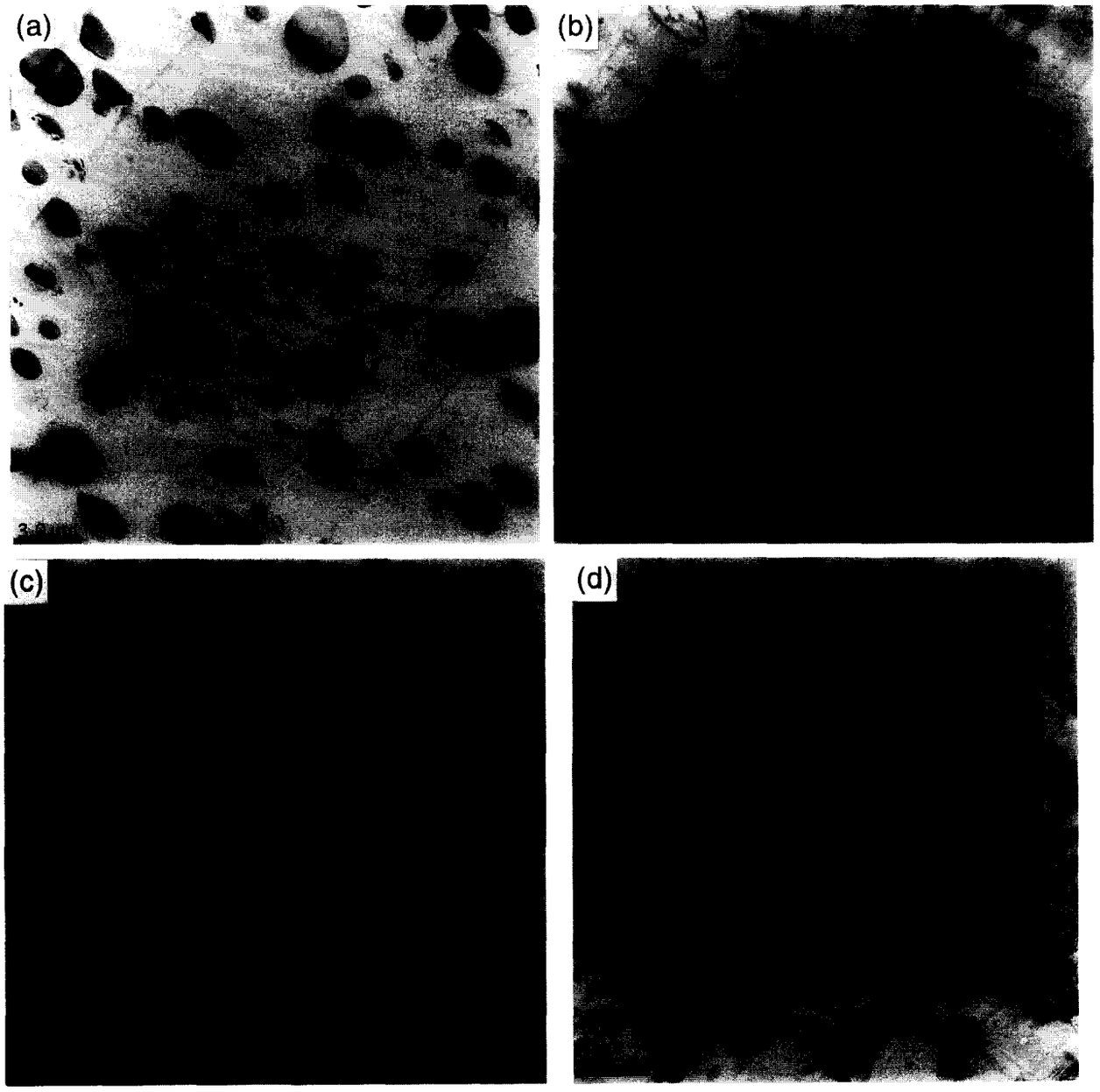

Figure 12 TEM photographs of 25/75 PA6/PC blends: (a) uncompatibilized; (b) with 5 phr; (c) with 10 phr; (d) with 15 phr of SEBS-gMA. PTA was used for staining PA6 in (a) and RuO_4 was used for staining SEBS-gMA in (b), (c) and (d)

viscosity of the PA6 phase is increased due to the reaction between PA6 and SEBS-gMA, which induces the phase inversion to the PA6 matrix.

The improvement of interfacial adhesion between the PA6 matrix and PC domains by the addition of SEBS-gMA can be proved by the observation of fracture surfaces with SEM. The uncompatibilized blend of 75/25 PA6/PC (*Figure 11a*) and the blend of the same composition with 5 phr of unmodified SEBS (*Figure 11c*) show that the rough fracture surfaces and voids are visible at the domain boundary, while the blends with SEBS-gMA (*Figure 11b*) shows a smooth fracture surface and the respective phases cannot be distinguished from the surface features. These differences of the surface feature represent the improved adhesion between the PA6 matrix and the PC domains by the reaction-induced phase formation of SEBS-gMA phase surrounding the PC domains.

The effect of the SEBS-gMA concentration on PC rich blends was also investigated by holding the PA6/PC ratio at 25/75. *Figure 12a* shows TEM photographs for an uncompatibilized blend of 25/75 PA6/PC where PTA has been used to stain the PA6 domains, while in *Figures 12b*, *12c* and *12d*, the morphologies of the blends of PA6/PC containing 5, 10 and 15 phr SEBS-gMA respectively are shown where the styrene blocks in SEBS-gMA are stained with RuO_4. The uncompatibilized blend shown in *Figure 12a* is characterized by the domains of PA6 clearly segregated from PC matrix and by voids on the domain boundary which are generated as a result of the delamination of PA6 domains from PC matrix. The blends of 25/75 PA6/PC with SEBS-gMA show the tendency that SEBS-gMA domains are occluded inside PA6 domains and the domain PA6 is dilated with increase of SEBS-gMA. At 5 phr incorporation of SEBS-gMA, the shape of the domains is nearly ellipsoidal (*Figure 12b*), and with the further addition of SEBS-gMA, the domains become irregular in shape as shown in *Figures 12c* and *12d*. *Figure 13* shows TEM photographs of PA6 domains with occluded SEBS-gMA inside them.

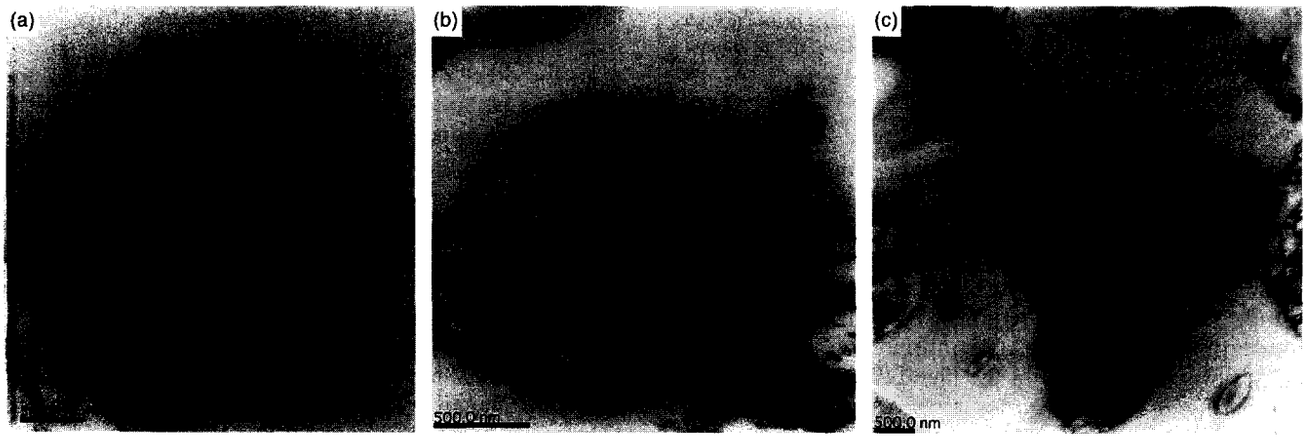

Figure 13 Higher magnification views of the domains of PA6 with occluded SEBS-gMA in the blends of 25/75 PA6/PC: (a) with 5 phr; (b) with 10 phr; (c) with 15 phr SEBS-gMA

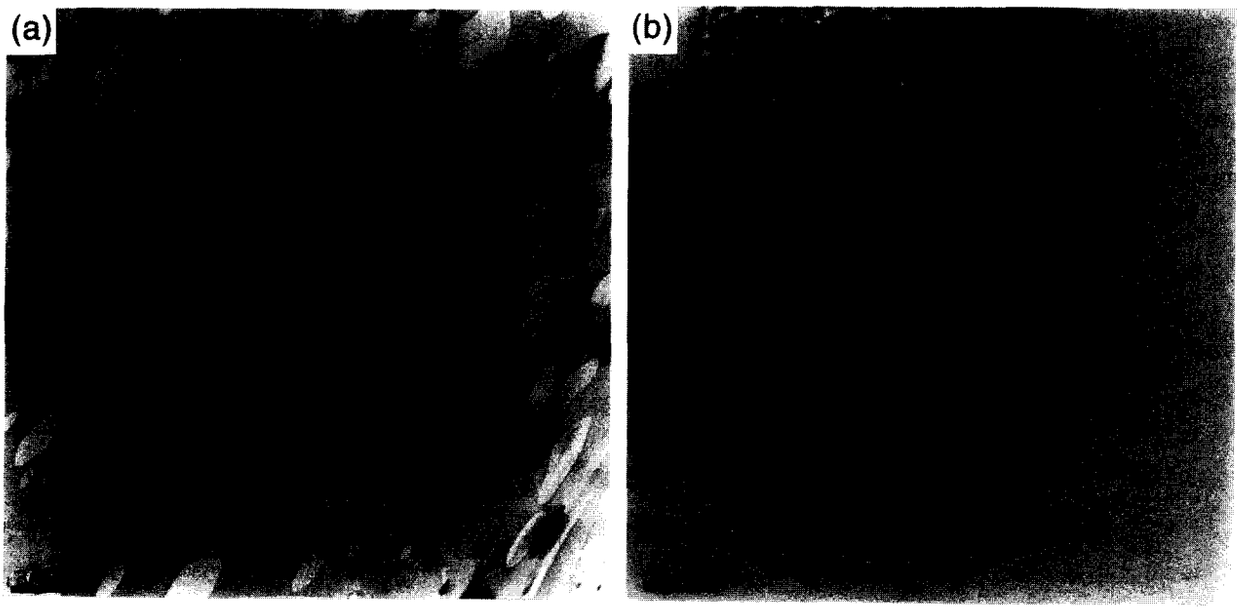

Figure 14 TEM photographs of 75/25/10 PA6/PC/SEBS blend. (b) is a higher magnification view of a SEBS domain showing the microdomain structure

Figure 15 TEM photograph of the domain boundary between PA6 and PC in 25/75/5 PA6/PC/SEBS-gMA where SEBS-gMA is stained with RuO_4

As shown in *Figure 13a*, in the blend containing 5 phr of SEBS-gMA, SEBS-gMA domains are dispersed in PA6 domains with a size of approximately 50 nm in diameter, which is comparable with that observed in the binary blends of PA6 with SEBS-gMA and PA6 rich ternary blends. In the blend with 10 phr SEBS-gMA, SEBS exists inside the domains both as continuous and dispersed phases (*Figure 13b*) and in the blend with 15 phr SEBS-gMA (*Figure 13c*), the domains occluded SEBS as continuous phase. On the contrary, the blends with unmodified SEBS show the structure in which PA6 phase and SEBS phase are separately dispersed in the PC matrix, as shown in *Figure 14a*. Neither of the dispersed components exhibits any tendency to spread onto the other. SEBS-gMA phases are stained dark with RuO_4 and these can also be identified by the higher magnification view of the domains which show microdomain structure of polystyrene (PS) and poly(ethylene-*co*-butylene) (PEB) as shown in *Figure 14b*. With increase of incorporation of SEBS-gMA, the extent of the graft formation of PA6 with SEBS-gMA is increased, which makes the PA6 domains highly viscous. This may cause the dilation of the domains and the formation of an irregular shape. The TEM photograph in *Figure 15* shows that SEBS-gMA phase exists on the interface between PA6 and PC but cannot reside within the PC phase. This indicates that SEBS-gMA is not miscible in PC but has affinity for PC. This information of SEBS-gMA phase on the domain boundary contributes to improving the interfacial adhesion between PA6 and PC, which results in disappearance of voids at the domain boundary.

Figure 16 illustrates the three distinct types of phase formation obtained in this study, which exhibit two dissimilar phases, dispersed in the third component. In the blends where PA6 forms the matrix, unmodified SEBS phase tends to attach to PC particles (*Figure 16a*), while SEBS-gMA encapsulates the PC particles (*Figure 16b*). On the other hand, in PC rich blends, the dispersed PA6 and SEBS phases form separate dispersed phases (*Figure 16c*). Morphology generation in three phase blends in which two dissimilar phases are dispersed in a third component has been discussed in terms of the interfacial tensions between the respective three polymers[29]. The tendency of one dispersed phase to spread onto the other dispersed phase can be predicted by the following equation, which has been obtained by rewriting Harkin's equation[30].

$$\lambda_{31} = \gamma_{12} - \gamma_{32} - \gamma_{13} \quad (1)$$

where γ_{12}, γ_{32} and γ_{13} are the interfacial tensions of components and λ_{31} is defined as the spreading coefficient for component 3 on component 1. The envelope formation of component 3 on component 1 will be observed for positive λ_{31} values. When λ_{31} and λ_{13} are both negative the dispersed phases will remain separated. Applying this equation to the phase formations as shown in *Figure 16*, it can be predicted that the phase formation in *Figure 16a* shows a nearly zero value of the spreading coefficients for SEBS on PC and the phase formation of *Figure 16b* shows a positive value, while the phase formation of *Figure 16c* exhibits negative values of λ_{31} and λ_{13} where λ_{31} is the spreading coefficient for SEBS on PC in PA6 matrix and λ_{13} is *vice versa*. Majumdar *et al.* have reported that the particle size of SEBS-gMA in the blends of PA6 is smaller by two orders of magnitude than the unmodified SEBS[14]. They mentioned that this drastic change in size

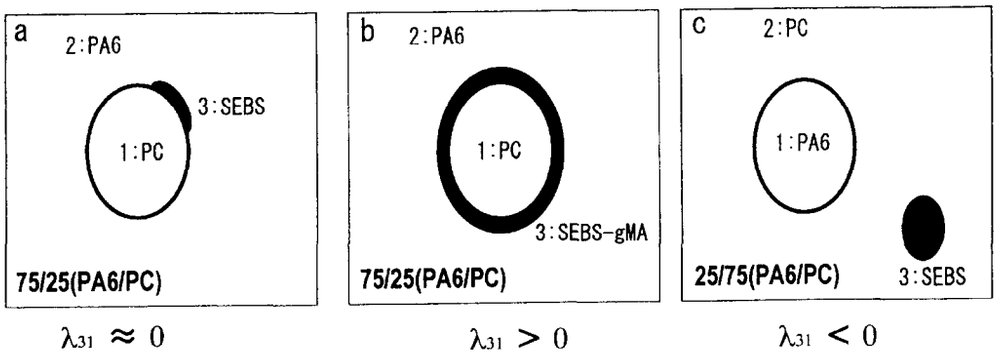

Figure 16 Schematic illustrations of the phase formations obtained from the ternary blends of (a) PA6/PC(75/25) with SEBS, (b) PA6/PC (75/25) with SEBS-gMA and (c) PA6/PC (25/75) with SEBS

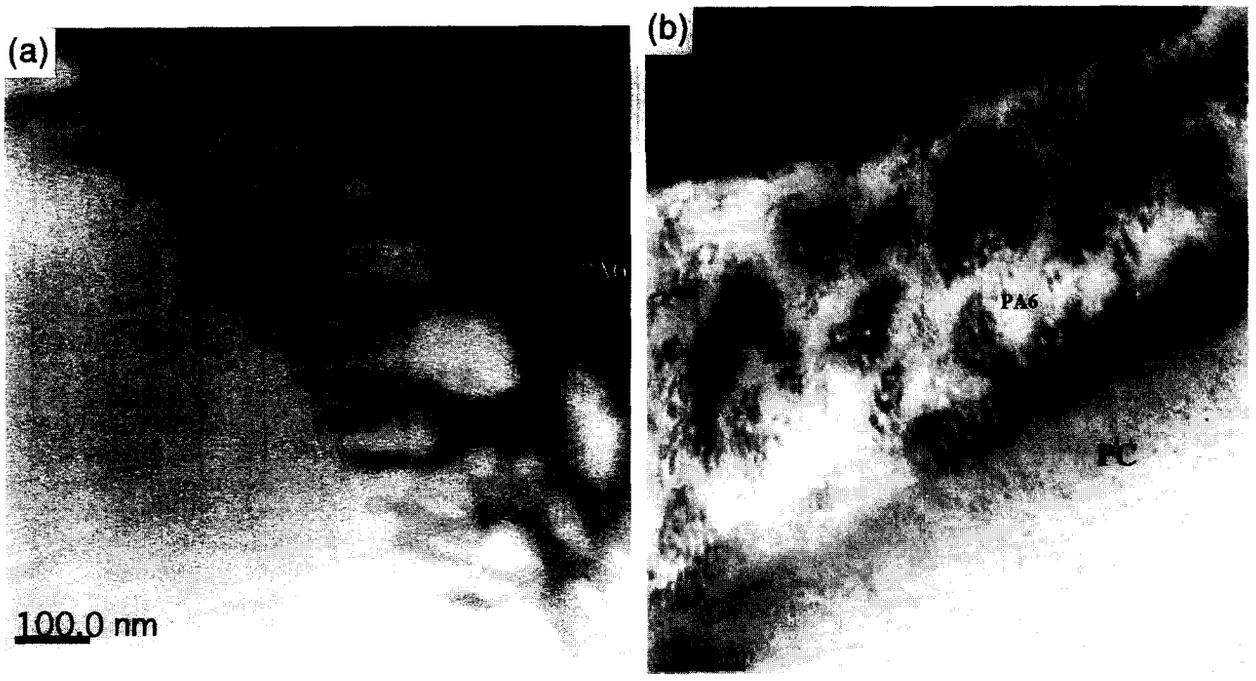

Figure 17 TEM photographs showing interfacial situation in the blends of 50/50/10 PA6/PC/SEBS-gMA in which (a) PA6 matrix has been stained with PTA and (b) SEBS-gMA domains have been stained with RuO_4

by the grafting reaction is not only due to the reduction of interfacial tension but also due to the steric hindrances against coalescence caused by the graft chains. Nevertheless, interfacial tension plays an important role in determining particle size in polymer blends. Although the interfacial tension between SEBS-gMA and PA6 is not obvious, with regard to the drastic decrease in particle size of SEBS-gMA, it is reasonable to expect the decrease of interfacial tension by the grafting reaction. This, therefore, leads to decrease of γ_{32} in equation (1), while γ_{12} (the interfacial tension of PC on PA6) and γ_{13} (PC on SEBS) are constant, and results in the increase of the spreading coefficient (λ_{31}). Thus, the change from the attached formation as illustrated in *Figure 16a* to envelope formation as shown in *Figure 16b* is induced by the reaction at the interface between SEBS and PA6.

The interfacial situation

The envelope formation of SEBS-gMA on PC particles in the PA6 rich blends have been found as described earlier in this paper by introducing the ESI mode and RuO_4 staining. It is worthwhile mentioning that the thickness of the phase on PC particles detectable by ESI mode and that by RuO_4 staining is different as shown in *Figure 8*. And also, by the staining with RuO_4, the interface of PC can be clearly identified, while in ESI mode it is diffused. The reason for that cannot be mentioned here, however, it may assumed that the phase observed in ESI mode includes both SEBS-gMA phase and the intermixed region. This can be assumed by taking into account that the contrast obtained with ESI mode represents the difference of element composition in each phase[20]. *Figure 17* shows the interfacial situation between PA6 matrix and a PC particle in the blends of 50/50/10 PA6/PC/SEBS-gMA. *Figure 17a* is a TEM photograph where PA6 matrix is stained with PTA and exhibits that the dispersed SEBS-gMA domains attach to the domain boundary. *Figure 17b* shows that styrene

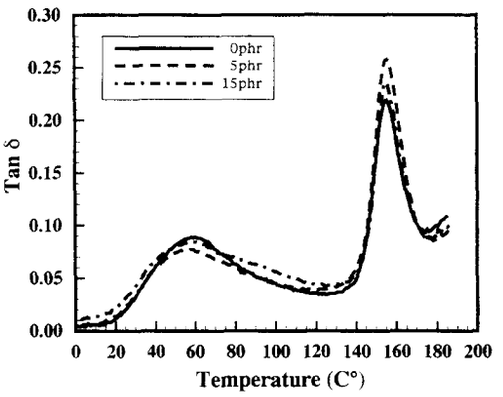

Figure 18 Tan δ trace obtained from d.m.a. measurements of 75/25 PA6/PC blends uncompatibilized and with 5 and 10 phr of SEBS-gMA

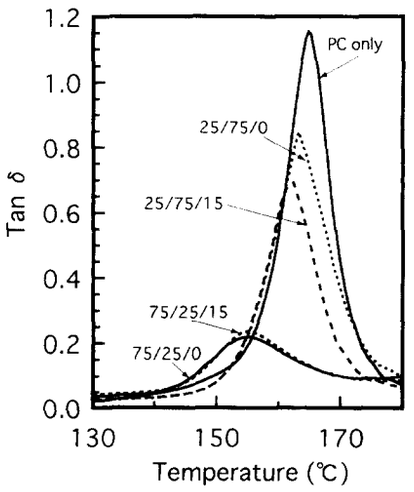

Figure 19 Tan δ trace associated with T_g of PC of pure PC, 75/25/0, 75/25/15, 25/75/0 and 25/75/15 PA6/PC/SEBS-gMA blends

blocks in SEBS-gMA are selectively stained with RuO_4. Careful observations of the domain boundary emphasizes the fact that the SEBS-gMA phase on the domain boundary shows the phase separation of rubbery (PEB) and plastic phases (PS), which leads to the properties of a thermoplastic elastomer. SEBS-gMA as an elastomer is expected to work as a stress absorber on the interface and as a coupling agent to improve the interfacial adhesion.

Dynamic mechanical analysis

PA6 and PC, although immiscible, can give rise to a large amount of chemical reactions during the melt blending with formation of block copolymers, degradation and crosslinking. Gattiglia *et al.* proposed possible reactions between the two polymers and mentioned that the aminolysis reaction:

$$\text{PA6}-\text{NH}_2 + \text{PC}-\text{O}-\text{COO}-\text{PC} \rightarrow$$
$$\text{PA6}-\text{NH}-\text{COO}-\text{PC} + \text{PC}-\text{OH} \qquad (2)$$

could be the leading reaction during the melt-mixing[3]. In this reaction, amine end groups of PA6 cleave the carbonate groups of PC which produces the copolymer and lower molecular weight of PC chains. The chemical reactions which occur during the mixing will cause deterioration of mechanical properties of the blends. In the ternary blends of PA6, PC and SEBS-gMA, two types of reaction will mainly occur, one of which is the graft reaction between PA6 and SEBS-gMA, and the other of which is the reaction shown in equation (2). These reactions and the extent of segmental mixing of SEBS-gMA will be reflected in the glass transition temperature (T_g) of the PC and PA6 phases. *Figure 18* shows the loss tan δ trace obtained from d.m.a. measurements as a function of temperature of the blends of 75/25 PA6/PC with various amount of SEBS-gMA. At every composition two T_g peaks are always present, clearly indicating the existence of two amorphous phases. No influences of added SEBS-gMA on the T_gs for both PC and PA6 phases are detectable. This tendency is also observed in the ternary blends of 25/75 and 50/50 with SEBS-gMA. *Figure 19* shows the loss tan δ peaks associated with the glass transition of the PC phase in pure PC, PC rich (25/75 PA6/PC) and PA6 rich blends (75/25 PA6/PC). This exhibited that the PA6 rich blends show considerable decrease of T_g for the PC phase than the PC rich blends show and also exhibited that the PA6 rich blends show the broadening of the peaks. In the blends of 75/25 PA6/PC, the amine concentration of PA6 terminal is so high that chemical reaction between PC and PA6, with reduction of the molecular weight of PC, takes place to a large extent. The low molecular weight species of PC, generated as a result of the chemical reaction between PA6 and PC, decrease the T_g for PC phase and broaden the molecular weight distribution. *Table 1* summarizes the T_g for the PA6 and PC phases taken from the peaks of tan δ trace. The decrease of T_gs for PA6 and PC phases from those of the respective pure polymers are detectable in all the blends, however, the effect of SEBS-gMA on the T_gs, for PC and PA6 phase is not detectable.

Together with the morphological analysis by TEM, the interfacial situation of PA6 and PC compatibilized with SEBS-gMA can be speculated as shown in *Figure 20*.

Table 1 T_gs of PA6 and PC phases obtained from tan δ peak in d.m.a. at 10 Hz

Formulation PA6/PC/SEBS-gMA	PA6 (°C)	PC (°C)
100/0/0	65	–
100/0/5	65	–
100/0/10	64	–
100/0/15	63	–
0/100/0	–	164
0/100/10	–	164
75/25/0	60	155
75/25/5	60	156
75/25/15	61	155
50/50/0	60	162
50/50/5	60	161
50/50/10	60	161
50/50/15	60	162
25/75/0	63	159
25/75/5	59	159
25/75/10	59	159
25/75/15	60	162

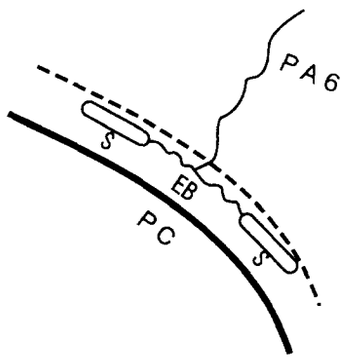

Figure 20 Speculative illustration of the location of SEBS-gMA on the interface between PA6 and PC

Table 2 Average diameters and statistical parameters for the PC domains in the blends of 75/25 PA6/PC obtained by image analysis of TEM photographs

Content of SEBS-gMA (phr)	Number-average particle diameter, $\bar{d}_n$ (μm)	Weight-average particle diameter, $\bar{d}_w$ (μm)	Distribution $\bar{d}_w/\bar{d}_n$	Standard deviation (μm)	Median (μm)
0	1.69	2.35	1.39	1.05	1.40
5	1.95	2.59	1.33	1.12	1.73
10	1.50	2.63	1.75	1.31	1.33
15	1.60	2.51	1.57	1.20	1.55
20	1.76	2.48	1.41	1.13	1.46

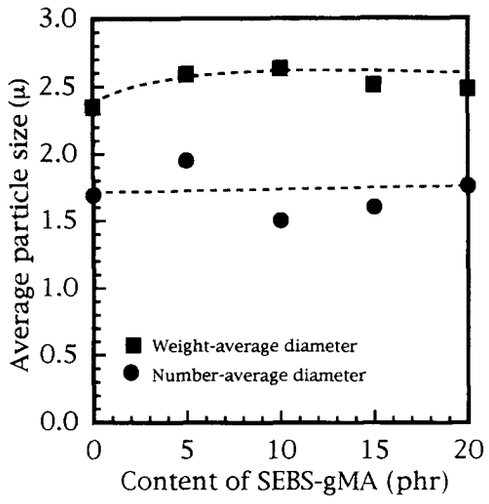

Figure 21 Average diameter of dispersed PC domains in the ternary blends of 75/25 PA6/PC with SEBS-gMA as a function of the content of SEBS-gMA

This indicates that the styrene blocks in SEBS are not miscible enough with the PC phase to reside within the PC phase. In this case, a drastic decrease of dispersed particles is not expected. *Table 2* summarizes the average diameter of PC domains and related statistical parameters obtained by image analysis of TEM photographs. When the image analysis was carried out, the fact that the particles in TEM images are not always cut through their centres was not taken into consideration, therefore, they appear to be smaller and show a more broad distribution than in reality. This, however, indicates that drastic decrease of PC domains cannot be achieved by the incorporation of SEBS-gMA as shown in *Figure 21*, where the number-average and weight-average particle size of PC are plotted against the amount of SEBS-gMA in the blends of 75/25 PA6/PC.

CONCLUSIONS

This work demonstrated that *in situ* reaction of amine terminals of PA6 and the maleated triblock elastomer, SEBS-gMA, induced the envelope formation of SEBS-gMA on PC-dispersed particles in PA6/PC/SEBS-gMA systems. The envelope formation of the SEBS-gMA phase on the domain boundary of PA6 and PC improved the interfacial adhesion and produced void-free blend materials. TEM observations revealed that SEBS-gMA on the interface exhibited the microdomain structure where the styrene hard segments form rod shapes and ethylene-butylene soft segments matrix. This structure is expected to show the property as an elastomer on the interface and to absorb the internal stress which is generated by the thermal shrinkage of PA6 and PC. Significant reduction of the dispersed particles has not been achieved by the addition of SEBS-gMA. This is because the SEBS-gMA phase is not miscible enough with PC to penetrate into the PC phase.

D.m.a. revealed that the reaction between PA6 and PC decreases the T_gs of the PA6 and PC phases, while the incorporation of SEBS-gMA cannot influence the T_gs, suggesting that the graft reaction of PA6 with SEBs-gMA cannot avoid the reaction between PA6 and PC which produces low molecular weight PC.

This paper also described how ESI is a powerful technique for investigation of the structure of heterogeneous polymer materials. Through use of the ESI mode with inelastically scattered electrons, the phase on the PC particles could have been visualized without staining. This demonstrates the amplification of contrast by the use of ESI which would be hardly detectable with conventional TEM. It appeared that the SEBS-gMA phases on PC particles visualized with ESI mode are thicker than with RuO_4 staining. It can be inferred that the phase with the ESI mode involves the intermixed region which contains the copolymer of PA6-PC and SEBS-gMA. New information offered by ESI may help to understand interfacial situations of polymer blend materials.

Future papers will relate the mechanical properties and morphology presented here and, also attempt the estimation of the contribution of interface adhesion to mechanical properties.

ACKNOWLEDGEMENTS

The authors thank Dr W. Probst, Mr N. Yamahira and Mr M. Ebisawa, Carl Zeiss, for the kindly advice on the Zeiss CEM902 operation and also thank Dr S. Yano, NIMC, for support on d.m.a. measurements.

REFERENCES

1 Gattiglia, E., Turturro, A. and Pedemonte, E. *J. Appl. Polym. Sci.* 1989, **38**, 1807
2 Gattiglia, E., Turturro, A., Pedemonte, E. and Dondero, G. *J. Appl. Polym. Sci.* 1990, **41**, 1411
3 Gattiglia, E., Turturro, A., La Mantia, F. P. and Valenza, A. *J. Appl. Polym. Sci.* 1992, **46**, 1887
4 La Mantia, F. P., Valenza, A., Gattiglia, E. and Turturro, A. *Intern. Polm. Processing* 1994, **3**, 240
5 Majumdar, B., Keskkula, H. and Paul, D. R. *Polymer* 1994, **25**, 5453
6 Majumdar, B., Keskkula, H. and Paul, D. R. *Polymer* 1994, **35**, 4263
7 Coran, A. Y. and Patel, R. *Rubber Chem. Technol.* 1983, **56**, 1045
8 Serpe, G., Jarrin, J. and Dawan, F. *Polym. Eng. Sci.* 1990, **30**, 553
9 Triacca, V. J., Ziaee, S., Barlow, J. W., Keskkula, H. and Paul, D. R. *Polymer* 1991, **32**, 1401
10 Tang, T., Li, H. and Huang, B. *Macromol. Chem. Phys.* 1994, **195**, 2931
11 Duvall, J., Sellitti, C., Myers, C., Hiltner, A. and Baer, E. *J. Appl. Polym. Sci.* 1994, **52**, 195
12 Duvall, J., Sellitti, C., Myers, C., Hiltner, A., Baer, E. and Myers, C. *Polymer* 1994, **18**, 3948
13 Gayload, N. G., Mehta, R., Kumar, V. and Tazi, M. *J. Appl. Polym. Sci.* 1989, **38**, 359
14 Oshinski, A. J., Keskkula, H. and Paul, D. R. *Polymer* 1992, **33**, 268
15 Oshinski, A. J., Keskkula, H. and Paul, D. R. *Polymer* 1992, **33**, 248
16 Takeda, Y., Keskkula, H. and Paul, D. R. *Polymer* 1992, **33**, 3173
17 Majumdar, B., Keskkula, H. and Paul, D. R. *Polymer* 194, **35**, 1386
18 Majumdar, B., Keskkula, H. and Paul, D. R. *Polymer* 1994, **35**, 1399
19 Majumdar, B., Keskkula, H. and Paul, D. R. *J. Appl. Polym. Sci.* 1994, **54**, 339
20 Bauer, R. in 'Methods in Microbiology' (Ed. F. Mayer), Academic Press, London, 1988, p. 113
21 Enerton, R. F. 'Electron Energy Loss Spectroscopy in the Electron Miscroscope', Plenum Press, New York, 1986
22 Disko, M. M. in 'Transmission Electron Energy Loss

Spectrometry in Materials Science' (Eds M. M. Disko, C. C. Ahn and B. Fultz), The Minerals, Metals and Materials Society, Pennsylvania, 1992, p. 1
23 Reimer, L. in 'Energy-Filtering Transmission Electron Microscopy' (Ed. L. Reimer), Springer, Heidelberg, 1995, p. 347
24 Kunz, M., Moller, M. and Cantow, H. J. *Makromol. Chem., Rapid Commun.* 1987, **8**, 401
25 Ban, L. L., Doyle, M. J., Disko, M. M. and Smith, G. R. *Polym. Commun.* 1988, **29**, 163
26 Ahn, C. C. and Krivanek, O. L. (Eds) 'EELS Atras', Gatan, Inc., Warrendale, 1983
27 Kortje, K. H. *J. Microscopy* 1994, **174**, 149
28 Trent, J. S., Scheinbeim, J. I. and Couchman, P. R. *Macromolecules* 1983, **16**, 589
29 Hobbs, S. T., Dekkers, M. E. J. and Watkins, V. H. *Polymer* 1988, **29**, 1598
30 Harkins, W. D. 'The Physical Chemistry of Surface Films', Reinhold Pub. Co., New York, 1952, p. 23